Dynamic ultrametricity in spin glasses

Ludovic Berthier,[1,2] Jean-Louis Barrat,[1] and Jorge Kurchan[3]
[1]*Département de Physique des Matériaux, Université C. Bernard and CNRS, F-69622 Villeurbanne, France*
[2]*Laboratoire de Physique, ENS-Lyon and CNRS, F-69007 Lyon, France*
[3]*PMMH, École Supérieure de Physique et Chimie Industrielles, F-75005 Paris, France*
(Received 9 June 2000; published 18 December 2000)

We investigate the dynamics of spin glasses from the ''rheological'' point of view, in which aging is suppressed by the action of small, nonconservative forces. The different features can be expressed in terms of the scaling of relaxation times with the magnitude of the driving force, which plays the role of the critical parameter. Stated in these terms, ultrametricity loses much of its mystery and can be checked rather easily. This approach also seems a natural starting point to investigate what would be the real-space structures underlying the hierarchy of time scales. We study in detail the appearance of this many-scale behavior in a mean-field model, in which dynamic ultrametricity is clearly present. A similar analysis is performed on numerical results obtained for a three-dimensional spin glass: In that case, our results are compatible with either that dynamic ultrametricity is absent or that it develops so slowly that even in experimental time-windows it is still hardly observable.

DOI: 10.1103/PhysRevE.63.016105 PACS number(s): 05.70.Ln, 75.10.Nr, 75.40.Mg

I. INTRODUCTION

A remarkable feature of mean-field models of spin glasses is the fact that pure states are organized in a hierarchical way. Given three equilibrium configurations (1,2,3) they determine a triangle whose sides are measured by the overlaps q_{12}, q_{13}, and q_{23}. If the configurations are chosen with the Gibbs weight then the two smallest overlaps are equal. This property, valid in the thermodynamic limit, defines an ultrametric space [1–3].

A first question to ask is whether ultrametricity exists in finite-dimensional systems. Numerically, this is investigated by searching low temperature ground states of very small systems, and looking for an ultrametric organization between them [4]. Experimentally, however, spin glasses are always out of equilibrium, and another relevant question may be what signatures of ultrametricity can be observable in a non-equilibrium system in the thermodynamic limit. In a relaxing (aging) mean-field system, it has been shown that ultrametricity would manifest itself in the dynamical behavior [5–8]: the correlation functions at three times $t_1 > t_2 > t_3 \gg 1$, $C(t_1,t_2)$, $C(t_2,t_3)$, and $C(t_1,t_3)$ satisfy the relation

$$C(t_1,t_3) = \min\{C(t_1,t_2), C(t_2,t_3)\}. \tag{1}$$

This property is often termed ''dynamic ultrametricity.'' A link between dynamic and static ultrametricity has been established by Franz *et al.* [9], who showed that the existence of an ultrametric solution from the dynamic point of view implies, under certain assumptions, the hierarchical organization of pure states in short-range systems. However, we are not aware of any report of dynamical ultrametricity [in the form (1)] in a simulated finite-dimensional system, or in experiments [8,10]. The reason may be that dynamic ultrametricity such as described by (1) is extremely difficult to observe numerically in an aging system [11]. Hence, for the three-dimensional (3D) Edwards-Anderson model, Franz and Ricci-Tersenghi [12] resorted to an indirect argument involving the coupling of replicas. Their simulation (together with their argument) then suggests a situation for three dimensions similar to the one observed in mean-field models.

From the experimental point of view, one obviously cannot use the method of [12]. Moreover, noise autocorrelations are extremely difficult to measure, but one can check the version of Eq. (1) involving the response functions [5]:

$$M^{\mathrm{TRM}}(t_1)|_{t_w=t_3} = \min\{M^{\mathrm{TRM}}(t_1)|_{t_w=t_2}, M^{\mathrm{TRM}}(t_2)|_{t_w=t_3}\}, \tag{2}$$

where $M^{\mathrm{TRM}}(t_a)|_{t_w=t_b}$ is the thermoremanent magnetization at time t_a when the field was cut off at time t_b. *Such a relation is not observed experimentally*. Indeed, the fit

$$M^{\mathrm{TRM}}(t_a)|_{t_w=t_b} \simeq \mathcal{M}\left(\frac{h(t_a)}{h(t_b)}\right) \tag{3}$$

works very well for suitable functions $h(t)$ [8], and it is *incompatible* with dynamic ultrametricity.

As has been often remarked, glassy dynamics can be studied in two complementary forms. One can study the relaxational aging system—and then the large parameter is the waiting time t_w—or one can drive the system in such a way that it becomes *stationary* [13–15]. In this second ''rheological'' form, the relevant parameter is the intensity of the driving force. Superconducting vortex systems with disorder have been studied this way [16,17]: in the presence of current the vortices are driven by a Lorentz force. In a spin glass, though less obvious to implement in experiments, the role of a ''stirring'' force can be played by nonsymmetric couplings [18–20].

Consider a system to which some nonconservative force of strength ε is added. It is by now well established that in a quench experiment, after some transient, the system becomes stationary. If the system is glassy, the relaxation times in the stationary regime will diverge as $\varepsilon \to 0$. (The time necessary

to achieve stationarity is of the same order, and will diverge as well—we will not study this in the present paper.) Indeed, we have that correlations decay for small ε as $C(t)=C_f(t)+C_s(t,\varepsilon)$, where the subindices denote ''fast'' and ''slow.'' [Recall that since we are in a stationary state, all the functions depend on a single time argument.] $C_f(t)$ represents the ''cage'' motion, or the fluctuations inside a domain, and is not affected by a small perturbation. $C_s(t,\varepsilon)$ is the slow motion, in which the system moves along the ''almost flat'' directions that are responsible for aging (e.g., structural rearrangements in a glass, domain wall motions in coarsening). The Edwards-Anderson parameter is given by $q \equiv \lim_{t\to\infty}\lim_{\varepsilon\to 0}C(t)$. A similar decomposition holds for $M^{\mathrm{TRM}}(t)$.

The dynamic ultrametricity discussed above becomes extremely simple in terms of the scaling of $C_s(t,\varepsilon)$ as $\varepsilon\to 0$. One possibility is indeed *simple scaling*:

$$C_s(t,\varepsilon)=f\left(\frac{t}{\overline{t}(\varepsilon)}\right), \tag{4}$$

where $\overline{t}(\varepsilon)\to\infty$ when $\varepsilon\to 0$, and f is a scaling function. Whenever Eq. (4) holds, we have that for two values of the correlation $C_1<C_2<q$:

$$\frac{t(C_1)}{t(C_2)} \underset{\varepsilon\to 0}{\to} \text{constant}, \tag{5}$$

where the relation $C_s(t)$ has been inverted to give $t(C)$. The behavior of Eqs. (4) and (5) is not the only possibility. An alternative would be that $C_s(t)$ is the sum of several terms of the type (4), each having a different scaling with ε. An extreme example of this is the *ultrametric law*, which for all $C_1<C_2<q$ results in

$$\frac{t(C_1)}{t(C_2)} \underset{\varepsilon\to 0}{\to} \infty. \tag{6}$$

The relationship of this property to Eq. (1) is immediate since, in the limit $\varepsilon\to 0$, one has $C(t(C_1)+t(C_2)) \sim C(t(C_1))=\min\{C(t(C_1)),C(t(C_2))\}$, which is the application of Eq. (1) to a stationary situation. This point is discussed in more detail in Sec. II C. The two following examples illustrate our discussion. Simple scaling is, for small ε,

$$C_s(t)\sim f\left(\frac{t}{\overline{t}(\varepsilon)}\right) \quad \Leftrightarrow \quad t(C)\sim\overline{t}(\varepsilon)j(C), \tag{7}$$

where $j(C)$ is the inverse function of f, while dynamic ultrametricity may be obtained with the small ε scaling

$$\ln[t(C)]\sim\overline{t}(\varepsilon)j(C) \quad \Leftrightarrow \quad C_s(t)\sim f\left(\frac{\ln(t)}{\overline{t}(\varepsilon)}\right), \tag{8}$$

where $\overline{t}(\varepsilon)$ may diverge with $\varepsilon\to 0$ as, for example, $\overline{t}(\varepsilon)\sim\varepsilon^{-a}$ and $j(C)$ is a positive decreasing function of C. Equation (8) clearly implies (6) and (1), and expresses the hierarchical scaling in a very straightforward way. In the stationary case, dynamic ultrametricity simply differs from simple scaling in that to make the correlation curves for different small ε collapse, *one has to rescale* $ln(t)$ *instead of t with a function of* ε.

Let us emphasize that such a simple statement of ultrametricity is not possible in the aging case. Consider, as an example, an aging system with correlations evolving as $C(\tau+t_w,t_w)=\ln(t_w)/\ln(t_w+\tau)$, which is *nonultrametric* since $C(t_3,t_1)=C(t_3,t_2)*C(t_2,t_1)$ [as opposed to Eq. (1)]. If we compare the time-differences $\tau(C)$ to reach two correlation values $C_1<C_2$, it is easy to find

$$\frac{\tau(C_1)}{\tau(C_2)}\sim(t_w)^{1/C_1-1/C_2} \underset{t_w\to\infty}{\to} \infty. \tag{9}$$

Hence, a criterion like (6) with t_w playing the role of the large parameter is *not* applicable in the aging case, and one has to go back to Eq. (1).

Our aims in this paper are the following.

(i) Within mean field, the solution exhibiting dynamical ultrametricity relies on an asymptotic analysis of the dynamical equations involving two-point correlation and response functions, which may thus be questionable. We will show that this analysis is indeed correct by solving numerically the dynamical equations governing the driven dynamics of a mean-field spin glass in the stationary regime. This is done on a very wide range of time scales, making us confident that the asymptotic solution is the correct one.

(ii) Since ultrametricity should hold strictly in the asymptotic limit of zero driving force (or equivalently in the infinite waiting time limit in the aging case), it is important to study also the preasymptotic regime to understand how ultrametricity gradually develops, and how a full hierarchy of time scales appears. We analyze then this preasymptotic regime in detail, thus characterizing the onset of ultrametricity.

(iii) Having the mean-field dynamical behavior in mind, it is very tempting to see if something similar happens in a finite-dimensional system. We have then performed a Monte Carlo simulation of the 3D Edwards-Anderson model with asymmetrical couplings. As is (unfortunately) usual in 3D spin glass simulations, our numerical results may be interpreted in two different ways. They are indeed compatible with an extremely slow appearance of dynamic ultrametricity, i.e., much slower than in the mean-field case. But an alternative view is that there is asymptotically only one relevant time scale, or, in other words, that dynamic ultrametricity is not present at all. In both cases the conclusion is that even if one assumes that ultrametricity is present, it has not fully developed for experimentally accessible time windows.

The paper is organized as follows. In the next section, the mean-field model under study is presented, and its preasymptotic behavior is detailed in Sec. III. Section IV presents our numerical results in three dimensions and Sec. V contains our conclusions.

II. A MEAN-FIELD DRIVEN SPIN GLASS

A. Model

We focus in this paper on a mean-field spin glass model first introduced in Ref. [21], where the statics was solved. The equilibrium dynamics was recently worked out [22]. It consists of a slight modification of the spherical p-spin model. We consider indeed N continuous variables s_i $(i=1,\ldots,N)$ interacting through the Hamiltonian

$$H=-\sum_{p=2}^{\infty}\sum_{j_1<\cdots<j_p} J_{j_1\cdots j_p}s_{j_1}\cdots s_{j_p}. \tag{10}$$

In this expression, the J's are random Gaussian variables, symmetrical about the permutation of $(j_1,\ldots,j_p)$ with mean zero and variance

$$\overline{J^2_{j_1\cdots j_p}}=\frac{p!J_p^2}{2N^{p-1}}, \tag{11}$$

so that the thermodynamic limit is well defined. A spherical constraint $\Sigma_{i=1}^N s_i^2(t)=N$ is, moreover, imposed on the spins. It is convenient to define also the function

$$g(C)\equiv\frac{1}{2}\sum_{p=2}^{\infty}J_p^2C^p. \tag{12}$$

The interesting case is when quadratic couplings are present together with quartic and/or higher-order interactions. It was shown that the model belongs then to the universality class of the Sherrington-Kirkpatrick model [21,22]: it has a continuous transition between a paramagnetic phase and a spin glass phase characterized by a full replica symmetry pattern and a nontrivial probability distribution of overlaps $P(q)$. Quantitatively, below the transition, one has

$$x(C<q)\equiv\int_0^C dq' P(q')=T\frac{g'''(C)}{2(g''(C))^{3/2}};\quad x(C>q)=1, \tag{13}$$

where q is the Edwards-Anderson parameter. This holds only if J_2 is big enough that $x'(C)=P(C)>0$. We consider in the following the combination of second- and sixth-order terms, keeping then only J_2 and J_6 different from zero. In this particular case, one has $T_c=J_2$ (independent of J_6). The positivity of $x'(C)$ gives, moreover, the inequality $J_6^2<J_2^2/15$.

B. Driven dynamics

To study the driven dynamics of the model, it is usual to consider a Langevin equation

$$\frac{\partial s_i(t)}{\partial t}=-\mu(t)s_i(t)-\frac{\delta H}{\delta s_i(t)}+\varepsilon f_i^{\rm nc}(t)+\eta_i(t). \tag{14}$$

As discussed in the Introduction, we take for the (nonconservative) driving force

$$f_i^{\rm nc}=\sum_{\substack{j_1<\cdots<j_{k-1}\\ j_1,\cdots,j_{k-1}\neq i}}\tilde{J}_i^{j_1\cdots j_{k-1}}s_{j_1}\cdots s_{j_{k-1}}. \tag{15}$$

The parameter ε controls the strength of the force. The couplings $\tilde{J}$'s in the driving force are random Gaussian variables, symmetrical about the permutations of $(j_1,\ldots,j_{k-1})$, with mean 0 and variance

$$\overline{\tilde{J}_i^{j_1\cdots j_{k-1}}\tilde{J}_i^{j_1\cdots j_{k-1}}}=\frac{k!}{2N^{k-1}};\quad \overline{\tilde{J}_i^{j_1\cdots j_{k-1}}\tilde{J}_{j_r}^{j_1\cdots i\cdots j_{k-1}}}=0. \tag{16}$$

These couplings are partially uncorrelated and contain thus an antisymmetrical part. This makes it impossible to write the driving force as the derivative of an energy. The parameter $\mu(t)$ ensures the spherical constraint and $\eta_i(t)$ $(i=1,\ldots,N)$ are random Gaussian variables with 0 mean and variance $2T$, where T is the temperature of the heat bath.

The dynamics of the model is better analyzed in terms of the autocorrelation function $C(t,t')\equiv\Sigma_i\langle s_i(t)s_i(t')\rangle/N$ and the response function $R(t,t')\equiv\Sigma_i\langle\delta s_i(t)/\delta\eta_i(t')\rangle/N$, since in the thermodynamic limit, $N\to\infty$, $C(t,t')$ and $R(t,t')$ verify closed Dyson equations [8]. The presence of the nonconservative force makes it possible to replace two-time functions $C(t,t')$ with single argument functions $C(t-t')$, and the following equations are obtained:

$$\frac{dC(t)}{dt}=-\mu C(t)+\int_0^t dt'\Sigma(t-t')C(t')+\int_0^\infty dt'[\Sigma(t+t')C(t')+D(t+t')R(t')],$$

$$\frac{dR(t)}{dt}=-\mu R(t)+\int_0^t dt'\Sigma(t-t')R(t'),$$

$$\mu=T+\int_0^\infty dt'[D(t')R(t')+\Sigma(t')C(t')],$$

$$D(t)\equiv g'(C(t))+\varepsilon^2\frac{k}{2}C(t)^{k-1},\quad \Sigma(t)\equiv g''(C(t))R(t). \tag{17}$$

These integrodifferential equations are associated with initial conditions $C(0)=1$, $R(0^+)=1$ and with the condition $R(t<0)=0$ (causality). The use of $C(-t)=C(t)$ in the derivation of Eqs. (17) made these equations noncausal in the time difference, as can be seen from the last integral in the equation for $C(t)$.

C. Asymptotic solution of the dynamical equations

In order to make the paper self-contained, and to set our notations, the asymptotic analysis of Eqs. (17) is now briefly recalled. A more detailed computation can be found in [5]. ''Asymptotic analysis'' means that the limit $\varepsilon\to0$ is taken.

The first step of the analysis consists in making the decomposition $C(t)=C_s(t)+C_f(t)$ and $R(t)=R_s(t)+R_f(t)$ between a fast and a slow part, and to derive the equations verified by each part. The equations for C_f and R_f are solved by making the ansatz that they satisfy the fluctuation-dissipation theorem (FDT) $TR_f(t)=-\mathrm{d}C_f(t)/\mathrm{d}t$. Taking the limit $t\to\infty$ gives then the following relation:

$$\mu+\frac{g'(q)-g'(1)}{T}=\frac{T}{1-q}, \tag{18}$$

where $q\equiv\lim_{t\to\infty}\lim_{\varepsilon\to 0}C(t)$ is the Edwards-Anderson parameter. The slow parts verify:

$$\begin{aligned}
\frac{\mathrm{d}C_s(t)}{\mathrm{d}t}&=-\mu C_s(t)+\int_0^t \mathrm{d}t'\Sigma_s(t-t')C_s(t')\\
&\quad+\int_0^\infty \mathrm{d}t'[\Sigma_s(t+t')C_s(t')+D_s(t+t')R_s(t')]\\
&\quad+\frac{g'(1)-g'(q)}{T}C_s(t)+\frac{1-q}{T}D_s(t),\\
\frac{\mathrm{d}R_s(t)}{\mathrm{d}t}&=-\mu R_s(t)+\int_0^t \mathrm{d}t'\Sigma_s(t-t')R_s(t')\\
&\quad+\frac{g'(1)-g'(q)}{T}R_s(t)+\frac{1-q}{T}\Sigma_s(t),\\
\mu&=T+\int_0^\infty \mathrm{d}t'[D_s(t')R_s(t')+\Sigma_s(t')C_s(t')]\\
&\quad+\frac{g'(1)-qg'(q)}{T},\\
D_s(t)&\equiv g'(C_s(t)),\quad \Sigma_s(t)\equiv g''(C_s(t))R_s(t).
\end{aligned} \tag{19}$$

The second step stems from the observation that once the first-order derivatives are dropped out (which is of course justified in the slow regime), the above equations become invariant under a reparametrization of time $t\to h(t)$. This suggests that C_s and R_s are related through a reparametrization-invariant formula, namely,

$$R_s(t)=-\frac{X(C_s(t))}{T}\frac{\mathrm{d}C_s(t)}{\mathrm{d}t}. \tag{20}$$

This amounts to an extension of the FDT to this nonequilibrium situation [14] by the introduction of an effective temperature $T_{\mathrm{eff}}(C)\equiv T/X(C)$. In the same spirit, the function f defining ''triangles'' is introduced:

$$C_s(t_1+t_2)\equiv f(C_s(t_1),C_s(t_2)). \tag{21}$$

Let us emphasize that the main assumption of the analysis is that the functions $X(C_s,\varepsilon)$ and $f(C_1,C_2,\varepsilon)$ have a continuous limit when $\varepsilon\to 0$. It is also convenient to define the function $\overline{f}$: $C_s(t_1)\equiv\overline{f}(C_s(t_2),C_s(t_1+t_2))$. This makes it possible to rewrite Eqs. (19) in such a way that the time disappears:

$$\begin{aligned}
0&=-\frac{T}{1-q}C_s+\frac{1-q}{T}g'(C_s)\\
&\quad+\frac{1}{T}\int_{C_s}^{q}\mathrm{d}C_s'g''(C_s')X(C_s')\overline{f}(C_s',C_s)\\
&\quad+\frac{1}{T}\int_{0}^{C_s}\mathrm{d}C_s'X(C_s')g''(C_s')\overline{f}(C_s,C_s')\\
&\quad-\frac{1}{T}\int_{0}^{C_s}\mathrm{d}C_s'g''(C_s')F[\overline{f}(C_s,C_s')],\\
0&=-\frac{T}{1-q}F[C_s]+\frac{1-q}{T}H[C_s]\\
&\quad+\frac{1}{T}\int_{C_s}^{q}\mathrm{d}C_s'g''(C_s')X(C_s')F[\overline{f}(C_s',C_s)],\\
F[C_s]&\equiv-\int_{C_s}^{q}\mathrm{d}C_s'X(C_s'),\\
H[C_s]&\equiv-\int_{C_s}^{q}\mathrm{d}C_s'X(C_s')g''(C_s'),
\end{aligned} \tag{22}$$

where Eq. (18) has been used.

The last step consists in computing explicitly X and f from Eqs. (22). This is done by introducing ''fixed points'' of f [5]. A fixed point $q^\star$ of f satisfies

$$f(q^\star,q^\star)=q^\star. \tag{23}$$

In the stationary context we are discussing, the physical meaning of such values of the correlation is very clear, since from the definition of f

$$q^\star=C_s(t)\Rightarrow C_s(2t)=f(C_s(t),C_s(t))=C_s(t), \tag{24}$$

which simply means that $q^\star$ is a *plateau* in the correlation function. Two such trivial fixed points are $q=0$ and $q=1$. It is then rather straightforward [5] to solve Eqs. (22). This gives $X(C)$ for $C\in[0,q]$,

$$X(C)=T\frac{g'''(C)}{2(g''(C))^{3/2}}, \tag{25}$$

and the matching with the FDT regime $(X(C>q)=1)$ determines q which satisfies $T=(1-q)\sqrt{g''(q)}$. The fact that $X(C)$ coincides with $x(C)$ [Eq. (13)] is a remarkable property of this class of mean-field spin glass models [5,9]. The properties of f are also obtained. It is first shown that $\forall\, C\in[0,q]$, $f(C,C)=C$, and there is hence a continuum of fixed points. Crudely speaking, it can be said that, in the asymptotic limit, each value of $C<q$ corresponds to a plateau value in the correlation function (in the sense that the correlation will not decay below this value in a finite time). This ultimately means that we will have a behavior as described by Eq. (6). It is also shown that

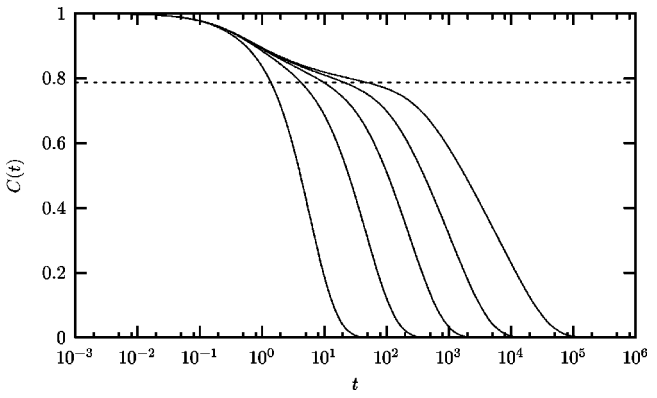

FIG. 1. Correlation function as a function of time for different values of the asymmetry for the mean-field model, at $T=0.25$. From left to right, $\varepsilon=2.25$, 0.8, 0.5, 0.35, 0.248. The horizontal dashed line is the value of the Edwards-Anderson parameter $q \simeq 0.787$.

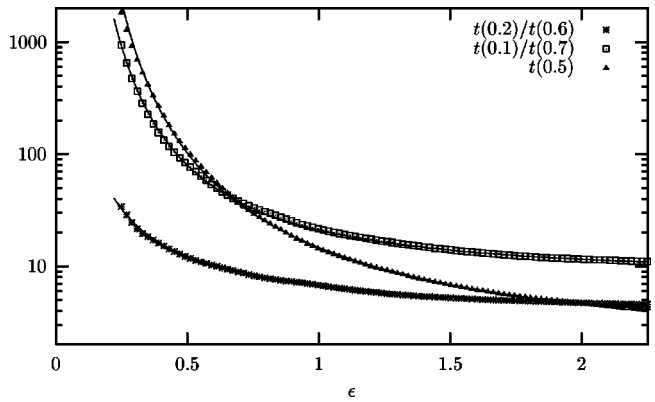

FIG. 2. Two different ratios of relaxation times as a function of the asymmetry for the mean-field model. Note that the vertical axis is in a logarithmic scale. Also plotted is the divergence of $t(0.5)$. The lines are fits of the form (27), with $j(C)$ as a fitting parameter.

$$\forall (C_1,C_2)\in[0,1]^2-[q,1]^2 \quad f(C_1,C_2)=\min\{C_1,C_2\}, \tag{26}$$

which is the ultrametric relation, as presented in the Introduction.

The conclusion of this section is that, apart from the trivial short-time behavior where $C(t)>q$ and FDT holds $X(C>q)=1$, the relaxation below q is characterized by a hierarchy of time scales and a nontrivial FDT $X(C<q)<1$.

III. ULTRAMETRICITY FROM DYNAMICAL CORRELATIONS

As stated in the preceding section, the asymptotic solution of the dynamical equations exhibits a ''many-plateau pattern,'' which is an unusual feature. To see how this asymptotic solution is approached, Eqs. (17) were solved numerically, in the particular case where $g(C)=C^2/2+C^6/30$, and $k=2$. We shall mainly work at $T=0.25=0.25T_c$, where the Edwards-Anderson parameter is $q\simeq 0.787$. To solve these equations, a combination of numerical methods of Refs. [23,24] has been used.

A. Hierarchy of time scales

The first element that is missed by the above analysis is the functional form of the correlation functions. They are depicted in Fig. 1, for different values of ε and for $T=0.25$. As expected, two different regimes are clearly present. For $C(t)>q$, the relaxation depends very weakly on the asymmetry, while for $C(t)<q$, the smaller the asymmetry, the slower the relaxation.

The main thing that cannot be determined analytically is the precise dependence of the relaxation times on the parameter ε that controls the strength of the asymmetry. The ''many-plateau pattern'' discussed above means that, in the preasymptotic regime (nonzero ε), the correlation will stay for a long, albeit finite, time around the same value. This characteristic time increases with decreasing C, as expressed by Eq. (6). In order to test this separation of time scales, we compute the ratio of relaxation times for two fixed values C_1 and C_2 of the correlation as a function of ε. Two such ratios are represented in Fig. 2, where it is clearly seen that they indeed diverge in the small asymmetry limit. A consequence is that the relaxation cannot be represented by a single time scale, but involves a full hierarchy of them. In particular, a stretched exponential fit such as the one proposed in [19] for the Sherrington-Kirkpatrick model with asymmetry can only be approximate.

The numerical solution of the dynamical equations suggests the following dependence for $C<q$:

$$t(C)\sim\exp[\overline{t}(\varepsilon)j(C)]; \quad \overline{t}(\varepsilon)\sim\varepsilon^{-0.65}. \tag{27}$$

In this expression, $j(C)$ is a positive decreasing function of the correlation. It plays the same role as in the example of the Introduction, Eq. (8). Numerically, $j(C)$ is consistent with a linear variation: $j(C)\simeq j(C=0)-bC$. For a fixed value C of the correlation, $t(C)$ grows faster than a power law of ε, as was noted in Ref. [19]. It also follows that

$$\frac{t(C_1)}{t(C_2)}\sim\exp[(j(C_1)-j(C_2))\overline{t}(\varepsilon)], \tag{28}$$

which means that the ratios of two time scales may be fitted by the same functional form (27) as the time scales themselves. This is also displayed in Fig. 2.

Let us note that the scaling (27) is very reminiscent of the ''creep'' regime scaling for vortex glasses [16], with the role of ε played by the current and C a measure of the average squared transverse displacements along the vortex.

The presence of this hierarchy of time scales in (27) implies that the correlation curves cannot be superimposed by rescaling the time. This is illustrated in Fig. 3, where the time is rescaled so that the curves meet at the value $C=0.3$. It can be seen that the curves are more and more horizontal around $C=0.3$, when the asymmetry is decreased. On the contrary, if we rescale the logarithm of the time to make the curves meet at $C=0.3$ (Fig. 4) we find that the curves tend to collapse. In other words: *shifting* $\ln(t)$ (as in

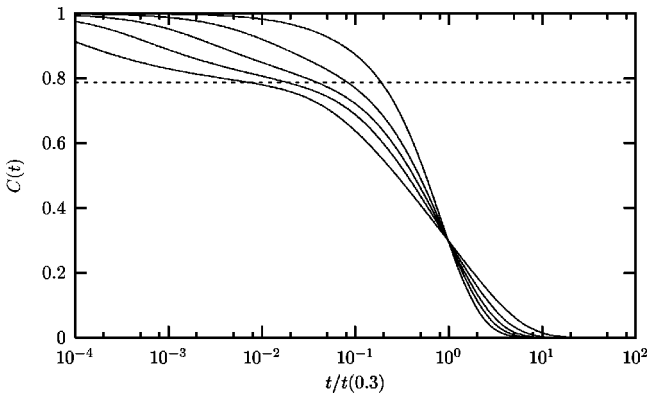

FIG. 3. Correlation function for the same values of the asymmetry as in Fig. 1. The time is rescaled by $t(0.3)$ so that curves superpose for $C=0.3$. Away from this value, there is no collapse for small ε.

simple scaling) does not make the curves collapse, while *stretching* $\ln(t)$ does. A similar picture would have been obtained by choosing any value $C\in[0,q]$.

This rescaling (or absence thereof) of the correlation functions in the driven dynamics of a spin glass is a direct and very simple test of dynamic ultrametricity. Let us emphasize again that, as already mentioned in the Introduction, this is not true for the aging regime.

B. Ultrametric relation and FDT

The function $f(C_1,C_2)$ introduced in Eq. (21) satisfies in the asymptotic limit the ultrametric relation (26). It is then natural to try to understand its preasymptotic behavior. A three dimensional view of this two-variable function is given in Fig. 5, for $\varepsilon=0.248$ (the slowest relaxation in Fig. 1). Also plotted in the plane (C_1,C_2) are the constant-f contours. These contours would be right angles in the limit of vanishing asymmetry.

To see how the function f evolves towards its asymptotic value [the ultrametric relation (26)], the evolution of the contours for different ε is represented in Fig. 6. These curves are very clearly evolving toward right angles, as expected from

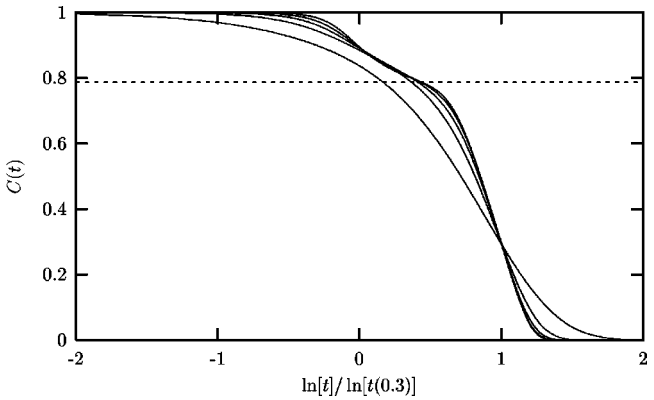

FIG. 4. Correlation function for the same values of the asymmetry as in Fig. 3, but here the *logarithm* of time is rescaled by $\ln[t(0.3)]$. The collapse for small ε is good.

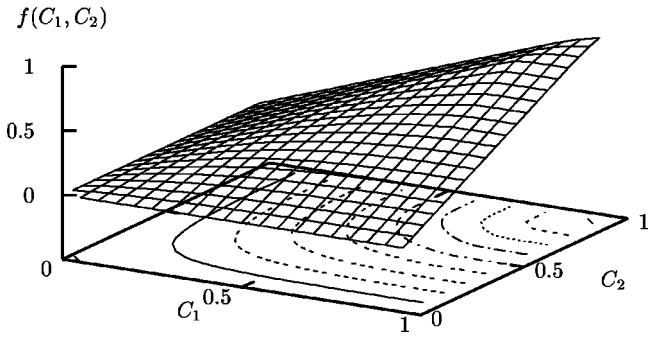

FIG. 5. Function f [Eq. (21)], for the value $\varepsilon=0.248$ in the mean-field model. The curves shown in the (C_1,C_2) plane are projections of horizontal cuts through the surface for $f=0.1,0.2,\ldots,0.9$.

the analysis of the preceding section.

It is interesting to compare these curves with the ones obtained from Ref. [15] for a system (p-spin with $p=3$) with a single time scale, i.e., without ultrametricity. The result is shown in Fig. 7, for correlations that evolve on a similar range of time scales to make the comparison relevant. In this case, the asymptotic analysis reveals that there exists asymptotically a function f defined as above, but it is not given by the ultrametric relation (26). The difference between the two systems is very clear from the comparison of Figs. 6 and 7: in the latter, the function f rapidly saturates to its asymptotic (nonultrametric) value.

To make the analysis of the mean-field dynamics complete, the usual plot [5] of the integrated response function $\chi(t)\equiv\int_0^t dt' R(t')$ as a function of the correlation function $C(t)$, parametrized by the time t, is done in Fig. 8. As expected from the above analytical results, the FDT holds for $C(t)>q$ and it is strongly violated for smaller values of the correlation. It is clear that in the limit of zero asymmetry, the analytic expression for the function $X(C)$ that generalizes the FDT to nonequilibrium situations will be recovered. The fact that the same limiting FDT violations happen in gently driven and aging systems has been suggested in Ref. [14],

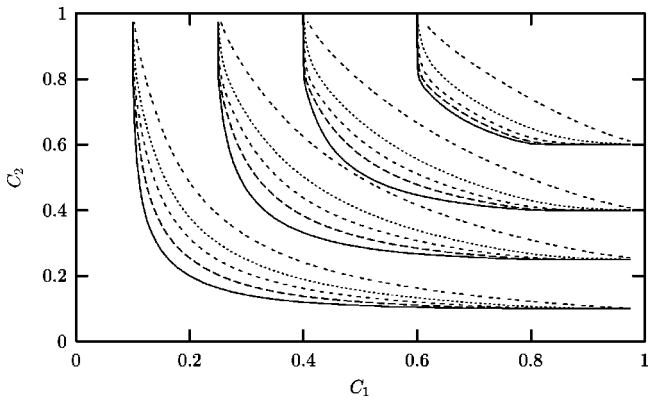

FIG. 6. Evolution of the projections for $f=0.1$, 0.25, 0.4 and 0.6 (see text) in the plane (C_1,C_2) for the values of the asymmetry as in Fig. 1: $\varepsilon=2.25$, 0.8, 0.5, 0.35, and 0.248. At each level f, the upper curve is for the larger asymmetry, and decreasing the asymmetry make the curves move towards right angles.

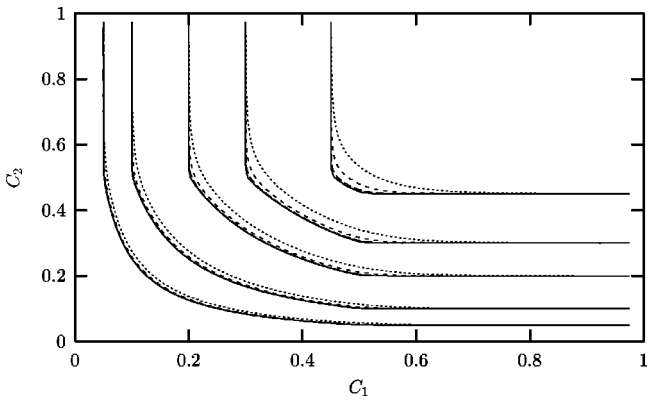

FIG. 7. Evolution of the projections for $f=0.05$, 0.1, 0.2, 0.3, and 0.45 (see text) in the plane (C_1,C_2) for the p-spin model (here $p=3$) studied in Ref. [15]. At each level f, the upper curve is for the larger asymmetry. In this case, the Edwards-Anderson parameter is $q\simeq 0.501$. The asymmetry (four values are represented) is chosen such that correlation functions cover a range of time scales similar to that of Fig. 1. When the asymmetry is decreased, the function evolves rapidly towards its limiting (nonultrametric) shape.

and we have verified here that this (mean-field) result holds also for systems with many time scales.

IV. SIMULATION OF THE 3D EDWARDS-ANDERSON MODEL

We turn now to the numerical results obtained for a 3D spin glass model, the results of the preceding sections being a guide to investigate its stationary driven dynamics. We use the same notations for quantities that play a similar role in the simulation and in the mean-field model, the distinction between the two cases being clear from the context.

A. Model and details of the simulation

The model under study is defined through its Hamiltonian

$$H=-\sum_{\langle i,j\rangle} J_{ij}s_i s_j, \tag{29}$$

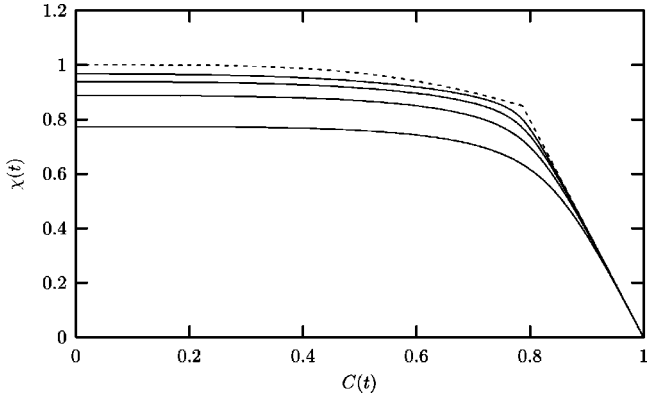

FIG. 8. Parametric plot of the susceptibility *vs* the correlation functions for $T=0.25$ and $\varepsilon=0.8$, 0.5, 0.35, and 0.248 for the mean-field model. The dashed curve is the analytic result, Eq. (25), for the limit $\varepsilon\to 0$.

where s_i $(i=1,\ldots,N)$ are $N=L^3$ Ising spins located on the sites of 3D cubic lattice of linear size L, with periodic boundary conditions. The sum $\langle i,j\rangle$ runs over nearest neighbors and the J's are chosen randomly from a bimodal distribution $J_{ij}=\pm 1$. The model has been extensively studied [10]: it exhibits a second order phase transition at the critical temperature $T_c=1.11\pm 0.04$ from a paramagnetic to a spin glass phase [25].

To drive the system, a coupling $\tilde{J}_{ij}$ is added on each link. The $\tilde{J}$'s are chosen from a bimodal distribution $\tilde{J}_{ij}=\pm\varepsilon$, and are antisymmetrical: $\tilde{J}_{ij}=-\tilde{J}_{ji}$. The small parameter ε controls the strength of the driving force. The spins are randomly sequentially updated through a standard Metropolis algorithm, and one Monte Carlo step represents N attempts to update a spin. Numerical results are presented for a linear size $L=20$ $(N=8000$ spins), where finite size effects are negligible for the time scales investigated here [26].

The temperature has been chosen such that the Edwards-Anderson parameter is comparable to the one of the mean-field case studied before. At $T=0.6\simeq 0.54T_c$, the Edwards-Anderson parameter was roughly estimated in an off-equilibrium simulation [with $\varepsilon=0$) through its dynamical definition $q=\lim_{t\to\infty}\lim_{t_w\to\infty}C(t,t_w)\sim 0.8$ (we had $q\simeq 0.787$ in the mean-field study]. Similarly, five different values of the asymmetry were studied: $\varepsilon=0.5$, 0.4, 0.3, 0.25, and 0.2, so that the range of time scales is comparable to the previous mean-field results. Remarkably, initial conditions are irrelevant, since a stationary state is reached after a time that depends on the intensity of the drive. As was already noted in Ref. [27], this is an unusual feature for glassy systems, where cooling procedures are known to be crucial. Moreover, stationarity makes it possible to average the correlation functions over different initial times, so that very few averages over the disorder have been necessary (typically 5), provided the first steps of the simulation are discarded. Stationarity has been carefully checked throughout the simulation.

B. Looking for ultrametricity

The dynamical quantity of interest is the spin-spin autocorrelation function, which in the TTI regime reads

$$C(t)\equiv\frac{1}{N}\sum_{i=1}^{N}\overline{\langle s_i(t+t_0)s_i(t_0)\rangle}. \tag{30}$$

The overline means that an average over disorder is performed, while $\langle\cdots\rangle$ stands for an average over different initial times t_0, all chosen in the TTI regime.

The autocorrelation functions for different values of the asymmetry at $T=0.6$ are represented in Fig. 9. As for the mean-field case, two different regimes are present. The short time relaxation towards $q\sim 0.8$ is very weakly affected by the driving force, while the time to relax towards zero dramatically increases when ε is lowered.

The crucial point is to look for the possible presence of the ultrametric relaxation pattern described in the preceding sections. We have seen above that a simple test of the presence of ultrametricity is the rescaling of the time. The same

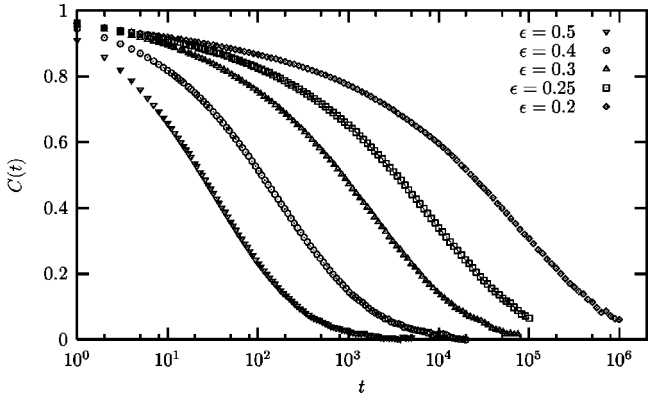

FIG. 9. Correlation functions for the 3D Edwards-Anderson model for different values of the asymmetry at $T=0.6$.

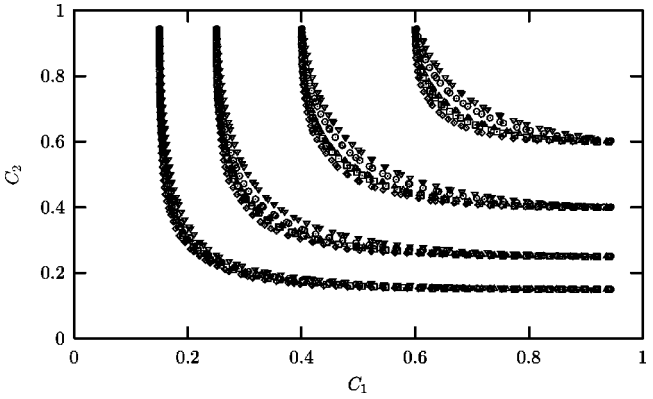

FIG. 11. Test of the function f for the 3D Edwards-Anderson model for $f=0.6$, 0.4, 0.25, and 0.15. The values of the asymmetry are the same as in Figs. 9 and 10, and are represented with the same symbols. This curve must be compared with Figs. 6 and 7.

rescaling that was done in Fig. 3 for the mean-field case is now performed for the 3D case in Fig. 10. Although not perfect, this rescaling works remarkably well for the smallest values of C. It is important to note that even if ultrametricity is absent, the values of correlation $1<C\lesssim q$ (which do not depend on the asymmetry) will not scale together with the $C<q$ portion of the curves. This may be a source of errors if the value of q is unknown. Thus, preasymptotic effects affect the quality of the rescaling in the region $C\sim q$, since it can be seen from Fig. 9 that the plateau is not completely developed. All these points may explain why the rescaling is good only for the smallest values of C.

However, a very slow flattening of the curves around the value $C=0.3$ cannot be completely excluded from this figure. But it is very clear that if there is a separation of time scales, then it *will become evident only if a much larger time window is analyzed*.

The second interesting quantity to study is the function $f(C_1,C_2)$ introduced in Eq. (21). Its evolution for different values of the asymmetry is depicted in Fig. 11, with the same construction as for Figs. 6 and 7. The function f indeed evolves, but very slowly when compared to the mean-field case. The quantitative behavior of f for the 3D model is more reminiscent of the $p=3$ case than of the mean-field spin glass case. Once again, this figure does not allow us to decide clearly between a limiting smooth—as it is for the $p=3$ case—or ultrametric f-function, because interesting things may happen on time scales that are inaccessible in our simulation time.

In our opinion, the important point that clearly emerges from the figures is that, on a given time window (we have four decades here), the relaxation does not appear to be typical of an ultrametric system and a single-time-scale description is very accurate. This may explain why dynamic ultrametricity has not been observed in aging experiments, which span some six decades $\sim$(100 Hz–10 h).

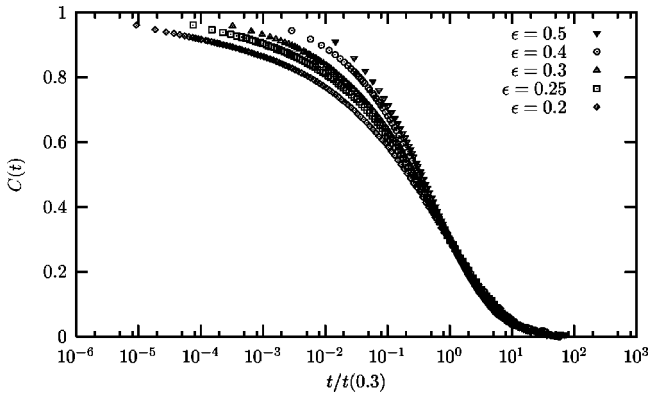

FIG. 10. Rescaling of the correlation functions of the Fig. 9. The rescaled time is such that all the curves meet at the value $C=0.3$. This figure must be compared with Fig. 3.

C. FDT

We have also investigated the way the FDT is violated in the driven 3D Edwards-Anderson model, since the mean-field theory suggests that these violations are the same as for an aging system. To our knowledge, there are no numerical confirmations of this prediction for spin glasses in the literature. For this purpose, correlation functions have to be compared to susceptibility curves. The correlation functions are taken from Fig. 9. The method of computing the susceptibility is now standard [28]. A stationary magnetic field h_i is applied at each site at time t_0. It is random in space, and we take it from a Gaussian distribution with mean 0 and variance $\overline{h_i h_j}=h_0^2\delta\{ij\}$. The staggered magnetization

$$m(t)\equiv\frac{1}{h_0 N}\sum_{i=1}^{N} h_i s_i(t) \tag{31}$$

is recorded for all $t>t_0$. In the linear response regime (we work with $h_0=0.1$, as in previous studies [10,28]), the susceptibility is obtained from $m(t)$ as $\chi(t)\simeq m(t)/h_0$. The results are averaged over several (from 50 to 300) realizations of the field, and over different initial times t_0. They are presented in Fig. 12.

The results for the violations of the FDT are clearly very similar to the mean-field ones. These curves exhibit two different regimes: for short times ($C\gtrsim q$), the FDT is well satisfied, whereas for longer times ($C\lesssim q$), it is violated. The

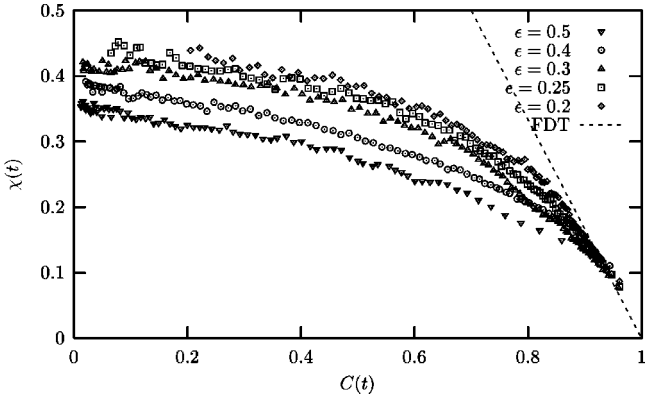

FIG. 12. Parametric plot of the susceptibility vs the correlation functions for the 3D model for different values of the asymmetry, at $T=0.6$. The curves saturate, in the small asymmetry limit, to a smooth limiting curve.

curves also clearly saturate to a smooth limiting curve in the small asymmetry limit. The shape of this limiting curve is compatible with the limiting nontrivial parametric curves that have already been found in simulations of 3D spin glasses in the aging regime [28]. The fact that both situations (aging and driven dynamics) exhibit the same kind of FDT violations deepens, in our opinion, the physical meaning of the quantity $X(C)$ (the so-called fluctuation-dissipation ratio) that can be extracted from this plot [9,14,29].

V. CONCLUSIONS

We have studied in this paper the behavior of spin glasses in a ''rheological'' setting, in which the dynamics is stationary and the control parameter is the strength of the driving force. We have checked the asymptotic analysis [5–7] for mean-field models through the numerical integration of the equations governing the dynamics. This has confirmed the presence of a full hierarchy of time scales in the relaxation of the correlation, Eq. (26), and a ''many-time-scale, many-temperature scenario'' [15]. This scenario can be seen as the dynamic counterpart of static ultrametricity. Simple scaling time dependencies, such as assumed in Ref. [19] could be justified for mean-field models only as an approximation valid in some time window, but do not hold strictly in the long time limit. Previous numerical studies of the aging dynamics of the Sherrington-Kirkpatrick model had pointed out the lack of simple t/t_w scaling [30], but did not investigate the presence of ultrametricity. Since there now exist powerful algorithms to solve dynamical two-time equations for long times [31], it would be interesting to have an analysis of the aging dynamics of a mean-field ultrametric model following the lines introduced in this paper.

For the 3D spin glass, our simulation suggests that the stationary driven dynamics is accurately interpreted within a single time scale relaxation pattern. We cannot decide whether our results imply an extremely slow appearance of ultrametricity (such that, even at experimental times, it is not fully observable), or its absence.

Whether transient or permanent, the single time scale relaxation obtained in our 3D simulation is in complete accordance with all the known numerical and experimental studies of the aging regime of 3D spin glasses [8,10,32]. In all known cases, two-time functions are indeed very well approximated by $M(t,t_w) \simeq \mathcal{M}(t/t_w)$, in contradiction to the dynamical mean-field theory, as we emphasized throughout the paper. It is interesting to note that the version of the ''droplet theory'' [33] which predicts the scaling $C(t,t_w) \sim \mathcal{C}(\ln(t)/\ln(t_w))$ fails also in reproducing experiments and simulations, since the logarithmic law is too slow.

Numerical results on 4D spin glasses also show that correlation functions are rather well represented by a t/t_w scaling in the aging regime [34], as is found in 3D. It would be extremely interesting to go back to the 4D simulations with asymmetrical couplings [20], or even to higher dimensions [35], to study precisely the stationary regime and see if, as in our simulation, there is a single time scale. It would be a disappointing result if all the richness of the ultrametric construction in spin glasses were a pure $D \to \infty$ feature.

The situation is made even more puzzling by the fact that this construction and the associated separation of time scales are often invoked to explain the results of temperature cycling experiments [8,36]. This is perhaps related to the difficulty in reproducing these experimental results with the 3D Edwards-Anderson model with numerical simulations [37].

[1] M. Mézard, G. Parisi, and M. A. Virasoro, *Spin Glass Theory and Beyond* (World Scientific, Singapore, 1987).

[2] M. Mézard, G. Parisi, N. Sourlas, G. Toulouse, and M.A. Virasoro, J. Phys. (France) **45**, 843 (1984); M. Mézard and M.A. Virasoro, *ibid.* **46**, 1293 (1985).

[3] R. Rammal, G. Toulouse, and M.A. Virasoro, Rev. Mod. Phys. **58**, 765 (1986).

[4] A.K. Hartmann, Europhys. Lett. **44**, 249 (1998); A. Cacciuto, E. Marinari, and G. Parisi, J. Phys. A **30**, L263 (1997); earlier references can be found in [1,3].

[5] L.F. Cugliandolo and J. Kurchan, J. Phys. A **27**, 5749 (1994); Philos. Mag. B **71**, 501 (1995).

[6] S. Franz and M. Mézard, Europhys. Lett. **26**, 209 (1994); Physica A **210**, 48 (1994).

[7] L.F. Cugliandolo, J. Kurchan, and P. Le Doussal, Phys. Rev. Lett. **76**, 2390 (1996); L.F. Cugliandolo and P. Le Doussal, Phys. Rev. E **53**, 1525 (1996).

[8] J.-P. Bouchaud, L. F. Cugliandolo, J. Kurchan, and M. Mézard, in *Spin Glasses and Random Fields*, edited by A.P. Young (World Scientific, Singapore, 1998), preprint cond-mat/9511042; E. Vincent, J. Hammann, M. Ocio, J.-Ph. Bouchaud, and L.F. Cugliandolo, in *Complex Behavior of Glassy Systems*, edited by M. Rubi (Springer-Verlag, Berlin, 1997), e-print cond-mat/9607224.

[9] S. Franz, M. Mézard, G. Parisi, and L. Peliti, Phys. Rev. Lett. **81**, 1758 (1998); J. Stat. Phys. **97**, 459 (2000).

[10] E. Marinari, G. Parisi, and J. J. Ruiz-Lorenzo, in *Spin Glasses and Random Fields*, edited by A.P. Young (World Scientific,

Singapore, 1998); preprint cond-mat/9701016.
[11] As far as we know, this was only attempted in [5], with rather inconclusive results.
[12] S. Franz and F. Ricci-Tersenghi, Phys. Rev. E **61**, 1121 (2000).
[13] H. Horner, Z. Phys. B **100**, 243 (1996); F. Thalmann, Eur. Phys. J. B **3**, 497 (1998); e-print cond-mat/0005162.
[14] L.F. Cugliandolo, J. Kurchan, and L. Peliti, Phys. Rev. E **55**, 3898 (1997).
[15] L. Berthier, J.-L. Barrat, and J. Kurchan, Phys. Rev. E **61**, 5464 (2000).
[16] M.P.A. Fisher, Phys. Rev. Lett. **62**, 1415 (1989); D.S. Fisher, M.P.A. Fisher, and D.A. Huse, Phys. Rev. B **43**, 130 (1991).
[17] T. Giamarchi and P. Le Doussal, in *Spin Glasses and Random Fields*, edited by A.P. Young (World Scientific, Singapore, 1998).
[18] J.A. Hertz, G. Grinstein, and S. Solla, in *Proceedings of the Heidelberg Colloquium on Glassy Dynamics and Optimization, 1986*, edited by J.L. van Hemmen and I. Morgernstern (Springer-Verlag, Berlin, 1987); G. Parisi, J. Phys. A **19**, L675 (1986); A. Crisanti and H. Sompolinsky, Phys. Rev. A **36**, 4922 (1987); **37**, 4865 (1988).
[19] G. Iori and E. Marinari, J. Phys. A **30**, 4489 (1997).
[20] E. Marinari and D.A. Stariolo, J. Phys. A **31**, 5021 (1998).
[21] T.M. Nieuwenhuizen, Phys. Rev. Lett. **74**, 4289 (1995).
[22] S. Ciuchi and A. Crisanti, Europhys. Lett. **49**, 754 (2000).
[23] K. Ng, J. Chem. Phys. **61**, 2680 (1974).
[24] M. Fuchs, W. Götze, I. Hofacker, and A. Latz, J. Phys.: Condens. Matter **3**, 5047 (1991).
[25] N. Kawashima and A.P. Young, Phys. Rev. B **53**, R484 (1996).
[26] A.T. Ogielski, Phys. Rev. B **32**, 7384 (1985).
[27] J.-L. Barrat and L. Berthier, Phys. Rev. E (to be published); e-print cond-mat/0003346.
[28] J.-O. Andersson, J. Mattsson, and P. Svedlindh, Phys. Rev. B **46**, 8297 (1992); S. Franz and H. Rieger, J. Stat. Phys. **79**, 749 (1995); E. Marinari, G. Parisi, F. Ricci-Tersenghi, and J.J. Ruiz-Lorenzo, J. Phys. A **31**, 2611 (1998); E. Marinari, G. Parisi, F. Ricci-Tersenghi, and J.J. Ruiz-Lorenzo, J. Phys. A **33**, 2373 (2000).
[29] S. Franz and M.A. Virasoro, J. Phys. A **33**, 891 (2000).
[30] H. Takayama, H. Yoshino, and K. Hukushima, J. Phys. A **30**, 3891 (1997); E. Marinari, G. Parisi, and D. Rossetti, Eur. Phys. J. B **2**, 495 (1998); A. Baldassarri, Phys. Rev. E **58**, 7047 (1998).
[31] B. Kim and A. Latz, e-print cond-mat/0005172; H. Horner (unpublished).
[32] J. Kisker, L. Santen, M. Schreckenberg, and H. Rieger, Phys. Rev. B **53**, 6418 (1996).
[33] D.S. Fisher, Physica D **107**, 204 (1997); D.S. Fisher and D.A. Huse, Phys. Rev. B **38**, 373 (1988).
[34] G. Parisi, F. Ricci-Tersenghi, and J.J. Ruiz-Lorenzo, J. Phys. A **29**, 7943 (1996).
[35] L.F. Cugliandolo, J. Kurchan, and F. Ritort, Phys. Rev. B **49**, 6331 (1994).
[36] L.F. Cugliandolo and J. Kurchan, Phys. Rev. B **60**, 922 (1999).
[37] M. Picco, F. Ricci-Tersenghi, and F. Ritort, e-print cond-mat/0005541.